

# Studying The Effect of Nano-dispersions ( $\text{Al}_2\text{O}_3$ ) on The Properties of A356 Hypo-eutectic Al-Si Cast Alloy

Abdallah M. Abdelkawy\*

Faculty of Engineering Cairo University, Giza, Egypt, aafatah\_meng@yahoo.com, aafatahmeng86@gmail.com

I. El Mahallawi

Faculty of Engineering, Cairo University, Giza, Egypt, ielmahallawi@bue.edu.eg

Tarek M. El Hossainy

Faculty of Engineering, Cairo University, Giza, Egypt, telhossainy@hotmail.com

## Abstract

Improving the strength to weight ratio is a target aimed by many researchers. Metal Matrix Nano Composites (MMNC) have recently emerged as a new generation of composites, where the addition of nano-sized particles leads to an increase in the strength not according to conventional Metal Matrix Composites rules. Aluminium matrix composites reinforced with nano-sized  $\text{Al}_2\text{O}_3$  particles are widely used for high performance applications such as automotive, aerospace and electricity industries. In this work a number of cast specimens made from hypoeutectic aluminium silicon alloy (A356) were cast with and without alumina ( $\text{Al}_2\text{O}_3$ ) nanoparticles at different pouring temperatures with stirring during the addition of nano-reinforcement. The microstructure of the new castings was studied using optical microscopy and scanning electron microscopic techniques. Also, the tensile strength, hardness and ductility were evaluated. The significant factors for the tensile strength were analysed using L4 orthogonal array and Analysis of Variance (ANOVA) techniques then building a model by Response Surface Methodology (RSM). The results obtained in this work show that adding alumina nanoparticles and pouring at different temperatures lead to an increase in the tensile strength and the hardness with less change in ductility.

Keywords: Nano-dispersion; MMNC; hypoeutectic; alumina; ANOVA; L4; RSM

Article history: Received June 6, 2014, Accepted December 4, 2014

## 1. Introduction

Saving energy for moving mechanical engineering applications has become on top of the agenda for many researchers seeking through the following two approaches:

1. Using new sources of renewable energy.
2. Optimizing the design parameters by choosing materials with high strength to weight ratio.

Within the latter concept, metal matrix nano-composites (MMNC) are tailored, depending on the application, to optimize the relation between the strength and weight. Many properties can be modified such as increased yield strength, tensile strength, young's modulus, fatigue strength, ductility,

creep resistance and improved thermal shock and corrosion resistance (Mazahery and Shabani, 2012). Casting is a prominent manufacturing method suitable for a great range of applications. The methods of casting fabrication of MMNC are classified according to the state of the material into liquid, liquid-solid (semisolid) and solid phases (El-mahallawi et al. 2012). Incorporating ceramic particles in the molten metal is the major challenge, mainly in terms of dispersing the particles uniformly in the matrix, while maintaining a strong bond between the ceramic particles and the matrix (Chatterjee and Mallick 2013). Semi-solid metal (SSM) casting produces final products with more homogeneous microstructures, less porosity and segregation that lead to large improvements in the mechanical properties. SSM also involves breaking

\* Corresponding author

the dendrites by electromagnetic forces or stirring during solidification (Yurko et al, 2003). J. Hashim et al, 2001, has concluded that some chemical and mechanical factors affect the wettability of ceramic particles by the molten metal and accordingly, some methods were suggested to enhance the wettability, such as employing mechanical force by stirring to overcome surface tension and improve wettability. EL-Mahallawi et al., 2010, studied the addition of different percentages of weight of  $Al_2O_3$  (1%, 2% and 4%) to the base alloy (A356) in the semi-solid state with mechanical stirring of the sludge on the mechanical properties of the composite, and have found that the ultimate tensile strength (UTS) increased for the nano-dispersed alloys compared to the monolithic alloys. It was also shown in their work that the max UTS and elongation percent were obtained at 2%  $Al_2O_3$ . Sajjadi et al., 2012, Conducted their experiments, similarly, on A356 using  $Al_2O_3$  with size  $20\mu m$  at weight percentages (1, 3, 5, and 7.5 wt. %) and 50nm at weight percentages (1, 2, 3, and 4%), pouring in both the fully molten and semi-solid states, rather, at  $700\text{ }^\circ C$  (liquid state) and at  $610\text{ }^\circ C$  (semi-solid state) with stirring. They found that yield strength and UTS were increased while the fracture strain decreased with increasing the nano-particle content. The state of molten metal had an effective role on the mechanical properties where compo-casting gave higher mechanical properties, which had been attributed to the enhanced wettability of the particles in compo-casting.

The aim of this search is correlate the manufacturing factors of the metal matrix composite affecting the mechanical properties; namely: the percentage of the nanoparticles in the cast sample (0 %, 2 wt. %), and the pouring temperature ( $630\text{ }^\circ C$  for the semi-solid state and  $700\text{ }^\circ C$  for the liquid state) by using ANOVA method on the UTS. The experimental results will be used to find the level of significant for each factor and Response Surface Methodology (RSM) to build a model able to predict the UTS in this range. Material and experimental procedure

## 2. Material and setup components

Primary material blocks of hypoeutectic aluminum silicon alloy A356 (fabricated in Helwan Company for nonferrous industries) were used as the main source for the matrix in this work with 6% Si, 0.255 Mg and 0.421 Fe. Alumina ( $Al_2O_3$ ) nanoparticles (NaBond technologies co. Limited) with average size 80 nm were used for reinforcement. The samples were fabricated by melting the alloy in an

electric resistance furnace with setup constructed for preparing the nano-dispersed alloys. The furnace consists of a heating system equipped with a control unit with two thermo couples for controlling the temperature in and out the crucible up to  $1200\text{ }^\circ C$ . The furnace also includes a stirring mechanism made of a motor of 3000 rpm attached to a stainless steel stirrer. A metallic mold made of cast iron with ten cylindrical mold cavities of diameter 20 mm and 150 mm in height were used for casting the test specimens.

### 2.1 Manufacturing

A charge of 1kg of A356 alloy was introduced to the crucible, which was then placed in the electric resistance furnace. The charge was heated up to a temperature slightly above  $700\text{ }^\circ C$  till it became completely liquid then the electric furnace was stopped. The melt was degassed with hexacholothane degasser tablets to dismiss the gases then the molten metal was left to cool to the specific temperatures (as shown in Table 1) at which the nanoparticles were added then the metal was stirred with stirrer at 1500 rpm for 2 min then the sludge was poured. The addition temperature, nanoparticles percent and pouring state are shown in the Table 1.

Table 1. The cast A356/ $Al_2O_3$  nanocomposite sample conditions.

Sample designation	Addition temperature $^\circ C$	Pouring state	$Al_2O_3$ %
A356/SSS	630	Semi-solid (SSS)	0
A356/LS	700	Liquid-state (LS)	0
MMNC/SSS	630	Semi-solid (SSS)	2
MMNC/LS	700	Liquid-state (LS)	2

### 2.2 Testing and characterization

The tensile strength was examined by using a tensile testing machine according to DIN 50125 (fig. 1). Both ultimate tensile strength and elongation percent were calculated. Three samples for each condition were examined and the average was considered to be the average ultimate tensile strength and elongation percent, respectively. The hardness was examined by using Rockwell hardness testing machine using 2.5 diameter ball and 62.5 kg. The average of 10 readings was considered as the average value of the hardness. The microstructure was investigated by optical microscope OLYMPUS DP12 after polishing the samples with 100, 400, 600, 1000, 1500, and 2500 grit paper, and etching by immersion in liquid with 95% of water and 5% Hydrofluoric

acid. Scanning electron microscopy (SEM) was used to investigate the cast sample MMNC/LS containing 2%  $\text{Al}_2\text{O}_3$  and poured at the liquid state.

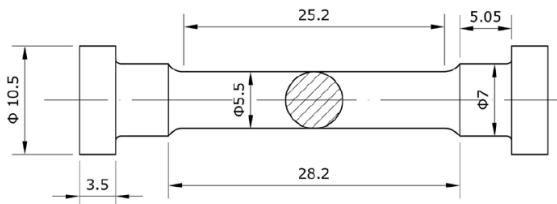


Fig 1 the standard dimensions for tension test samples.

### 3. Results and discussion.

#### 3.1 Mechanical properties

Fig. 2 shows the ultimate tensile strength, the hardness and the elongation percent for the tested alloys. From this figure, it is found that the increase in the tensile strength in the case of MMNC poured at semi-solid state is 10% and 22% for the MMNC poured at the liquid state compared to the monolithic A356 alloy poured from the liquid state. The elongation percent for the MMNC poured from the liquid state is 65% higher than the monolithic samples. As for the case of MMNC poured from the semi-solid state, the ductility is nearly constant possibly due to agglomeration of the nanoparticles. Fig 2(c) shows that the hardness is constant for all the cast samples. This increase in UTS and ductility is a result of dispersion strengthening and grain refinement, where the particles and the matrix have the same crystalline phase (FCC) and the interfacial energy is lower so, the matrix/particle interface has high dense-packed structure and able to prevent any cracks and the dispersion of the nanoparticles effectively hinders the dislocation motion (Koch, 2006).

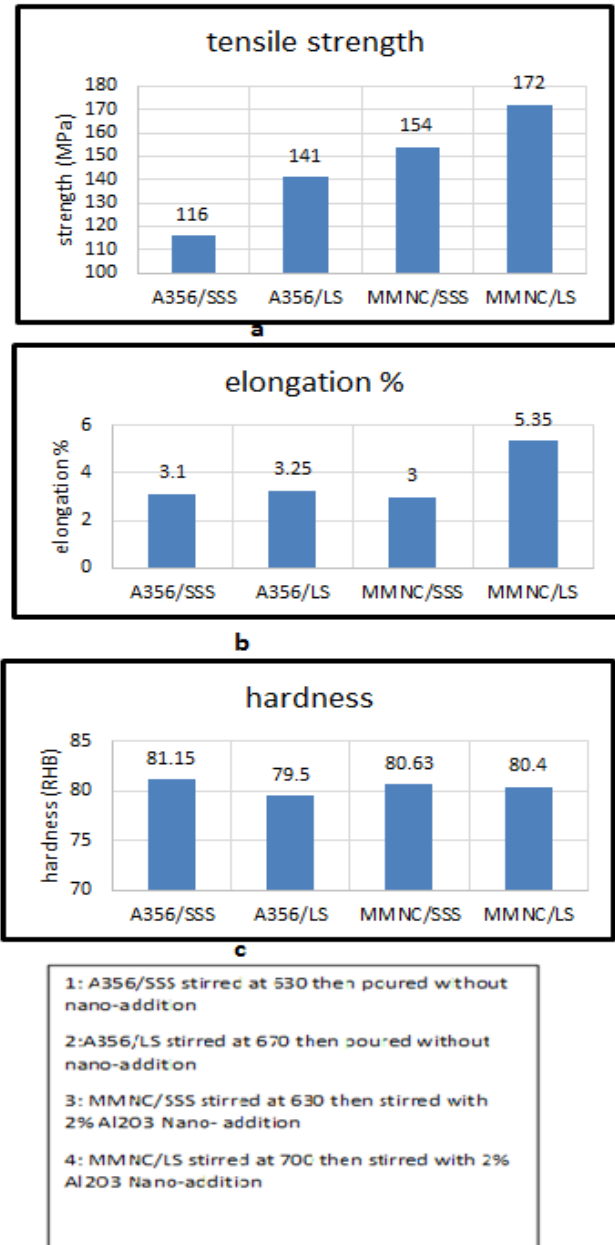


Fig. 2. The mechanical properties of the cast A356/ $\text{Al}_2\text{O}_3$  nanocomposite: (a) the tensile strength, (b) the elongation percent, and (c) the hardness in HRB

#### 3.2 Microstructure

Fig. 3 shows the microstructure for A356/SSS, A356/LS, MMNC/SSS and MMNC/LS. The microstructures show that the  $\alpha$ -grains change their morphology in the case of the semi-solid state to a globular shape compared to the dendritic shape in case of the liquid state (Dey et al., 2006).

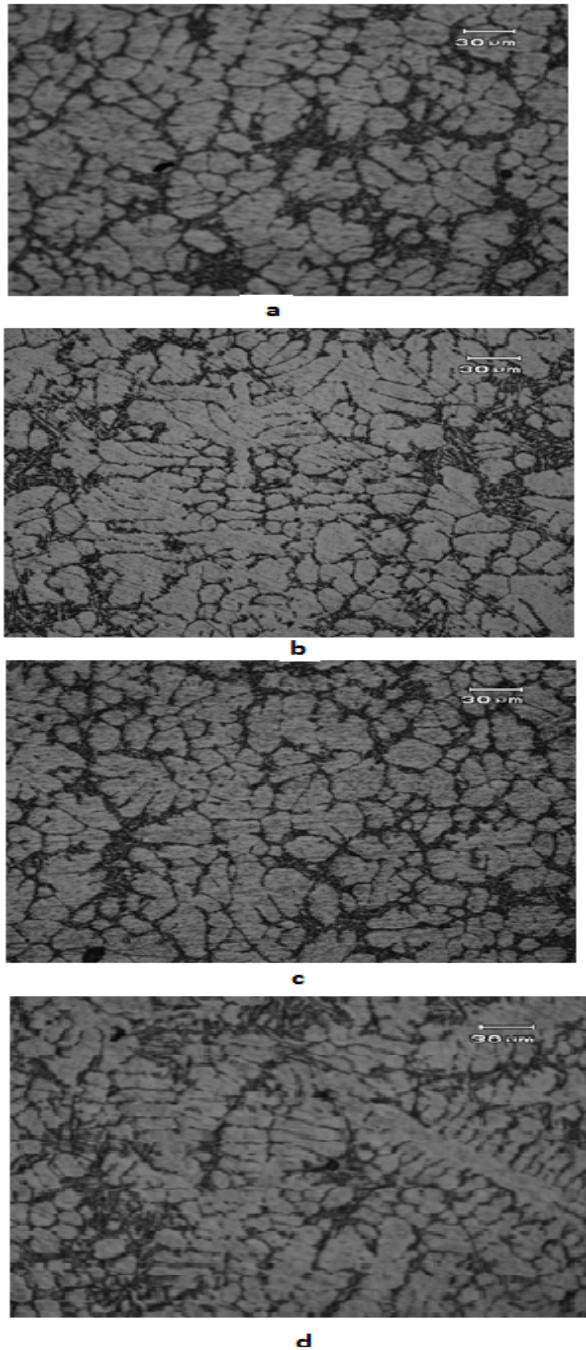


Fig. 3. Micrograph showing the microstructure of (a) A356/SSS, (b) A356/LS, (c) MMNC/SSS and (d) MMNC/LS.

Where, the fragmentation of the dendrites to globular is occurred either by bending of the dendrite arms then the liquid enters into their high-angle grain boundaries or by melting the root of the dendrite arms due to solute enrichment (Reisi and Niroumand, 2012). The globular crystal structure improves the fluidity, eliminates the defects such as solidification segregation, shrinkage, porosity and improves the

mechanical properties (Xin et al., 2010). The porosity (appearing in the microstructure) in case of MMNC/SSS is possibly the reason for the reduced ductility compared to previous studies. Fig. 4(a) shows the SEM micrograph for MMNC/LS. The figure shows incorporation of agglomerations of nanoparticles of  $\text{Al}_2\text{O}_3$  in the matrix of the alloy. Fig. 4(b) shows the EDX quantitative analysis of the particulate-agglomerates in MMNC/LS confirming the presence of oxide particles of  $\text{Al}_2\text{O}_3$  in the alloy.

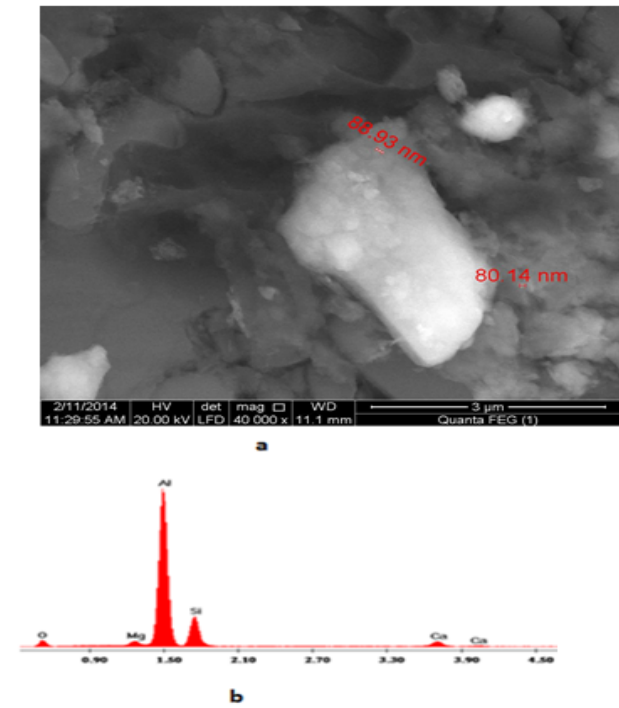


Fig. 4. SEM micrograph and EDX quantitative analysis of aluminum silicon alloy A356 reinforced by nano- sized  $\text{Al}_2\text{O}_3$  particles: (a) The SEM micrograph for MMNC/LS, and (b) The EDX quantitative analysis for MMNC/LS.

#### 4. The statistical analysis for the tensile strength.

##### 4.1 Application of ANOVA techniques

The L4 orthogonal array was used to apply the ANOVA technique of the response of tensile strength. Table 2 shows the L4 for two factors (nano percent and the temperature of addition the nanoparticles, each one has two levels) and the tensile strength. Table 3 shows the ANOVA data components as the variables, statistical summation (SS), the degree of freedom (DOF), and variance and the calculated Fisher factor for each factor (F cal.).

Table 2. L4 orthogonal array.

No.	Nano %(A)	Addition temp. °C(B)	UTS(Mpa)
1	0	700	141
2	0	630	116
3	2	700	172
4	2	630	154

Table 3. The ANOVA table.

Variables	SS	DOF	variance	Fcal
Nano%	1190	1	1190	97.16
Add. Temp	462	1	462	38.5
Error	12	1	12	
Total	1664	3		

Where the tabulated fisher value ( $F_{0.10,1,1}$ ) at 90% is 39.9 and ( $F_{0.050,1,1}$ ) at 95% is 161. Nano-particles reinforcement percent is significant at 90% level and temperature is nearly significant at 90%.

#### 4.2 Modelling by RSM.

The model of tensile strength is built by using Response Surface Methodology (RSM). The model relates nanoparticles percent and stirring temperature.

$$UTS = 29.75 + 11.7 * nano\% + 0.164 * add.temp^{0.99} \quad (1)$$

Table 4 shows the predicted, measured values of tensile strength, error and error percent. The model quality is equal to 94.5 %.

Table 4. Predicted, measured values of tensile strength, error and error percent.

No.	$Al_2O_3$ %	Add. temp °C	measured	predicted	error	Error %
1	0	700	141	137	3.7	2.67
2	0	630	116	126.6	9.6	8.22
3	2	700	172	160.6	11.3	6.5
4	2	630	154	150	3.9	2.5

Fig. 5(a) shows a graphical relation of both stirring temperature and nanoparticles percent to ultimate tensile strength which is obtained by equation (1). Fig. 5(b) shows the comparison between the predicted and measured values of UTS.

#### 4.3 The model verification

The model developed through this work was verified by testing the experimental work conducted through other investigations on similar alloy and semi-solid casting conditions (El-mahallawi et al., 2012), (Sajjadi, Ezatpour, and Parizi, 2012). The first sample

(1% nano-reinforcement, 630 °C nano-particles addition) had measured UTS 143MPa and 145MPa model value with 1.4 % error percent. The second sample (2% nano-reinforcement, 630 °C nano-particles addition) had measured UTS 160 MPa and 156 MPa model value with 2.18 % error percent. The results show good agreement with the model, as the difference between the model results and the experimental reported results where error percent of only 2.2% maximum

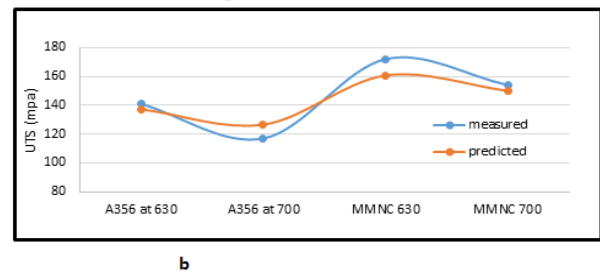
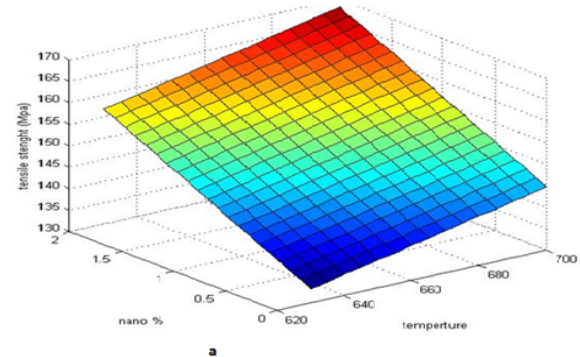


Fig. 5. (a) The relation between temperatures, nanoparticles percent with the tensile strength and (b) Comparison between the measured and predicted values.

## 5. Conclusion

The main results obtained from this work aiming to study the effect of addition nanoparticles of alumina  $Al_2O_3$  powder to molten A356 alloy at different temperatures on the microstructure and the tensile strength at fixed stirring conditions are:

- 1- The UTS increases after adding nanoparticles of  $Al_2O_3$  to A356 alloy.
- 2- Stirring and pouring at the semi-solid state changes the microstructure from dendritic shaped to granular shaped microstructure.
- 3- The ANOVA technique shows that the temperature and nanoparticles percent are significant parameters at a level of 90% for a model built with RSM method of 95% quality.
- 4- The model must be used in the same range of the parameters used to build it.

## References

- Mazahery, Ali, Mohsen Ostad Shabani, 2012. Characterization of Cast A356 Alloy Reinforced with Nano SiC Composites, Transactions of Nonferrous Metals Society of China 22(2), pp 275–80. [http://dx.doi.org/10.1016/S1003-6326\(11\)61171-0](http://dx.doi.org/10.1016/S1003-6326(11)61171-0).
- El-Mahallawi, I. et al. 2012. Influence of Al<sub>2</sub>O<sub>3</sub> Nano-Dispersions on Microstructure Features and Mechanical Properties of Cast and T6 Heat-Treated AlSi Hypoeutectic Alloys, Materials Science & Engineering A; 556, pp 76–87. <http://dx.doi.org/10.1016/j.msea.2012.06.061>.
- Chatterjee, Subhranshu, Amitava Basu Mallick, 2013. Challenges in Manufacturing Aluminium Based Metal Matrix Nanocomposites via Stir Casting Route, Materials Science Forum, 736, pp 72–80.
- Yurko, James A., Martinez, Raul A., Flemings, Merton C., 2003. Commercial Development of the Semi-Solid Rheocasting (SSRTM) Process, Metallurgical Science and Technology.” 21(1), pp 10–15.
- Hashim, J., Looney, L., Hashmi, M. S. J., 2001. The Wettability of SiC Particles by Molten Aluminium Alloy, Journal of Materials Processing Technology, 119 (1-3), pp 324–28.
- El-Mahallawi, I. S. et al. 2010. Influence of Nanodispersions on Strength–Ductility Properties of Semisolid Cast A356 Al Alloy.” Material Science and Technology 26(10), pp 1226–1231.
- Sajjadi, S. A., Ezatpour, H. R., Torabi Parizi, M., 2012. Comparison of Microstructure and Mechanical Properties of A356 Aluminum Alloy / Al<sub>2</sub>O<sub>3</sub> Composites Fabricated by Stir and Compo-Casting Processes, Materials and Design 34, pp 106–11. <http://dx.doi.org/10.1016/j.matdes.2011.07.037>.
- Koch, Carl C., 2006. Nanostructured Materials: Processing, Properties, and Applications, William Andrew Inc.
- Dey, A. K., Poddar, P., Singh, K.K., Sahoo, K. L., 2006. Mechanical and Wear Properties of Rheocast and Conventional Gravity Die Cast A356 Alloy, Materials Science and Engineering 435, pp 521–529.
- Reisi, M., Niroumand, B., 2012. Initial Stages of Solidification during Semisolid Processing of a Transparent Model Material, Materials Chemistry and Physics 135(2-3), pp 738–48. <http://dx.doi.org/10.1016/j.matchemphys.2012.05.053>.
- Xin, L. I. N. et al., 2010. Morphological Evolution of Non-Dendritic Microstructure during Solidification under Stirring, Transactions of Nonferrous Metals Society of China 20(3), pp s826–s831.